Asian Journal of Control, Vol. 00, No. 0, pp. 1–10, Month 2011
Published online in Wiley InterScience (www.interscience.wiley.com) DOI: 10.1002/asjc.0000

ADAPTIVE HARMONIC STEADY-STATE DISTURBANCE REJECTION WITH FREQUENCY TRACKING

S. Pigg and M. Bodson

ABSTRACT

The paper is concerned with the rejection of sinusoidal disturbances of unknown frequency acting at the output of unknown plants. Disturbance rejection is based on an adaptive harmonic steady-state (ADHSS) algorithm combined with a magnitude/phase locked-loop (MPLL) frequency estimator. The harmonic steady-state method assumes that the plant can be approximated by its steady-state frequency response. For high-order plants such as those encountered in active noise and vibration control (ANVC), this assumption greatly reduces the number of parameters and enables online estimation of the plant response using simple algorithms. The paper shows that when the MPLL is integrated with the ADHSS algorithm, the two components work together in such a way that the control input does not prevent frequency tracking by the MPLL and so that the order of the ADHSS can be reduced. Thus, the addition of the MPLL allows disturbances of unknown frequency to be considered without significantly increasing the complexity of the original ADHSS. After analyzing the reduced-order ADHSS in the ideal case, the equations describing the complete system are considered. The theory of averaging is used to gain insight into the steady-state behavior of the algorithm. It is found that the system has a two-dimensional equilibrium surface such that the disturbance is exactly cancelled. A subset of the surface is proved to be locally stable. Extensive active noise control experiments demonstrate the performance of the algorithm even when disturbance and plant parameters are changing.

Key Words: adaptative control, disturbance rejection, unknown plant, frequency estimation

I. Introduction

The paper considers an adaptive algorithm for the rejection of sinusoidal disturbances of unknown/time-varying frequency acting on unknown/time-varying systems, with particular focus paid to issues arising in *active noise and vibration control* (ANC, AVC, or ANVC) applications. This problem is a difficult one for which few practical solutions exist in the literature, especially considering that ANVC plants are often of high order, and sometimes with significant delay. Time-varying plants are not very frequent, but are occasionally encountered. For example, [10] discusses the cancellation of high-frequency noise in headsets, and reports that small movements in the headset position can create significant changes in the secondary path dynamics (*i.e.,* the plant). In particular, due to the short wavelength associated with high-frequencies, the phase of the frequency response may change by more than 90 degrees with small movements of the headset. A new adaptive feedforward controller for the rejection of periodic disturbances can be found in [3]. Unlike [3], sytems of the pure feedback type are considered in this paper.

S. Pigg received his Ph.D. in Electrical and Computer Engineering from the University of Utah and currently works as a design engineer. [scott_pigg@hotmail.com].
M. Bodson is a Professor with the Department of Electrical and Computer Engineering at the University of Utah.
50 S. Central Campus Dr. Rm 3280 [bodson@ece.utah.edu].

When the plant is known (possibly measured in a preliminary experiment with white noise), a typical solution in ANVC is based on the well-known filtered-X LMS (FXLMS) algorithm. Therefore, it is natural that methods for time-varying plants [4] [13] to provide online plant estimation for this algorithm. While the adaptive methods have been shown to work, they are computationally intensive and require the injection of a significant amount of white noise to provide sufficient excitation. Stability of the algorithms is also rarely addressed due to the difficulty in decoupling the two components of the algorithm. [12] analyzes the FXLMS algorithm with online secondary path modeling and narrowband disturbances, and derives a closed form expression for the mean squared error of the cancellation error in the presence of estimation errors. It is shown that stability requires that the phase of the frequency response of the secondary path must be within $90°$ of the estimated path's frequency response.

A more recent and original approach can be found in [6]. The algorithm extends the known frequency/unknown system algorithm of [5] by adding frequency estimation. The algorithm has been shown to work under certain random variations in the unknown parameters. We have found in simulations that a large amount of measurement noise was sometimes needed to insure stability. [6] is based on a steady-state approximation of the plant's response to sinusoidal signals. This paper follows a similar approach, but uses different control and frequency estimation algorithms. An adaptive harmonic steady-state (ADHSS) algorithm for disturbances of known frequency [8] is used with a magnitude/phase locked loop approach for frequency estimation [11]. In [1], the MPLL algorithm is used for the rejection of disturbnces consisting of two unknown frequency components when the system's plant is known. After investigating a reduced-order ADHSS, the overall system consisting of the reduced-order ADHSS and the MPLL is considered. Equilibrium points of the system are found that ensure perfect rejection of the disturbance in ideal conditions, and local stability is guaranteed under certain conditions. Finally, multiple active noise control experiments with variations in plant and disturbance parameters demonstrate the performance of the algorithm under challenging conditions.

II. Problem Statement

Consider the feedback system shown in Fig. 1. The output of the plant

$$y(t) = P(s)[u(t)] + p(t) \tag{1}$$

is fed back in order to determine the control signal $u(t)$ needed to reject the sinusoidal disturbance $p(t)$. The notation $P(s)[(\cdot)]$ represents the time-domain output of the system with transfer function $P(s)$. $P(s)$ is assumed to be a bounded-input-bounded-output stable linear time-invariant system, but is otherwise unknown. Although the plant is fixed in the analysis, experiments have shown that the use of adaptation allows the plant to vary significantly over time [8]. The compensator C is generally a nonlinear and time-varying control law consisting of a parameter identification scheme and a disturbance cancellation algorithm.

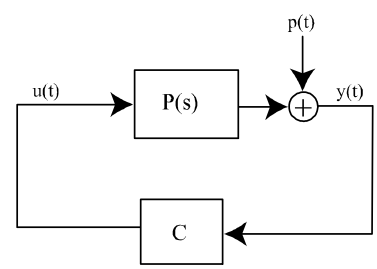

Fig. 1: Feedback control system.

The disturbance is written as

$$p(t) = m^* \cos(\alpha_1^*(t)) \tag{2}$$

where

$$\alpha_1^*(t) = \alpha_1^*(0) + \int_0^t \omega_1^* d\tau \tag{3}$$

and ω_1^* is the true frequency of the disturbance. m^* is an unknown magnitude. The control signal is written as

$$u(t) = \theta_c \cos(\omega_1 t) + \theta_s \sin(\omega_1 t) = w_1^T(t)\theta \tag{4}$$

where

$$\theta = \begin{pmatrix} \theta_c \\ \theta_s \end{pmatrix}, \quad w_1 = \begin{pmatrix} \cos(\alpha_1(t)) \\ \sin(\alpha_1(t)) \end{pmatrix} \tag{5}$$

and

$$\alpha_1(t) = \int_0^t \omega_1(\tau) d\tau \tag{6}$$

ω_1 is an estimate of the disturbance.frequency. In [8], an HSS algorithm was used for determining an appropriate control vector θ when the plant $P(s)$ is unknown and the disturbance frequency is known exactly, i.e. $\omega_1 = \omega_1^*$. In this paper, it is shown how the HSS algorithm of [8] can be simplified and extended for consideration of the case where ω_1^* is not known.

III. Adaptive algorithm for known frequency

3.1. ADHSS algorithm

We first review the *adaptive harmonic steady-state algorithm (ADHSS)* of [8] for the rejection of sinusoidal disturbances of known frequency affecting unknown plants. The disturbance was expressed in terms of its cos and sin components as

$$p(t) = w_1^T(t)\pi \tag{7}$$

with

$$\pi = \begin{pmatrix} p_c \\ p_s \end{pmatrix} \tag{8}$$

where p_c and p_s are unknown parameters. Note that this expression is equivalent to (2) for

$$\begin{pmatrix} p_c \\ p_s \end{pmatrix} = m^* \begin{pmatrix} \cos(\alpha_1^*(0)) \\ -\sin(\alpha_1^*(0)) \end{pmatrix} \tag{9}$$

$$\omega_1 = \omega_1^* \tag{10}$$

For fixed parameters, the steady-state output of the plant was written

$$y_{ss}(t) = w_1^T(t)\,(G\theta + \pi) \tag{11}$$

where

$$G = \begin{pmatrix} P_R & P_I \\ -P_I & P_R \end{pmatrix} \tag{12}$$

and P_R, P_I are the real and imaginary parts of the plant's frequency response evaluated at ω_1, *i.e.,* $P(j\omega_1) \triangleq P_R + jP_I$. It was shown that (11) can be rewritten as

$$y_{ss}(t) = W^T(t,\theta)x^* \tag{13}$$

where

$$W(t,\theta) = \begin{pmatrix} \theta_c & \theta_s & 1 & 0 \\ \theta_s & -\theta_c & 0 & 1 \end{pmatrix}^T w_1(t) \tag{14}$$

is a so-called regressor matrix and

$$x^* = \begin{pmatrix} P_R & P_I & p_c & p_s \end{pmatrix}^T \tag{15}$$

is a vector of unknown parameters. From the linear expression (13), a gradient algorithm given by

$$\dot{x} = -gW(t,\theta)\left(W^T(t,\theta)x - y\right) \tag{16}$$

was used to obtain an estimate x of the unknown vector x^*. The control input was determined from the estimate x using

$$\theta(x) = -\begin{pmatrix} x_1 & x_2 \\ -x_2 & x_1 \end{pmatrix}^{-1} \begin{pmatrix} x_3 \\ x_4 \end{pmatrix} \tag{17}$$

3.2. Properties of the ADHSS system

Justification for the steady-state approximation and further stability properties were obtained in [8] through application of averaging theory. A significant result of the application of averaging theory is the fact that the nonzero eigenvalues of the linearized averaged system around an equilibrium point lie in the open left-half plane if and only if

$$x_1x_1^* + x_2x_2^* > 0 \tag{18}$$

For the reverse sign, the eigenvalues lie in the open right half plane. The stability condition means that the difference of phase between the estimated plant model and the true plant dynamics must be less than 90°. The condition is the same as for the filtered-X LMS algorithm, but the difference is that the instability for phase difference greater than 90° is only local, and the nonlinear dynamics ensure that trajectories originating close to the unstable equilibrium points eventually converge to the stable subset of the equilibrium surface [8].

3.3. Effect of a frequency error

Unfortunately, the adaptive algorithm does not tolerate well a frequency error. To explain this characteristic, reconsider the disturbance as given by (2). ω_1 and α_1 continue to be the frequency and phase estimates used by the adaptive algorithm, and its equations remain unchanged. Note that the disturbance can be written as

$$\begin{aligned} p(t) &= m^* \cos(\alpha_1(t) + (\alpha_1^*(t) - \alpha_1(t))) \\ &= w_1^T(t)\pi(t) \end{aligned} \tag{19}$$

where

$$\pi(t) = \begin{pmatrix} p_c(t) \\ p_s(t) \end{pmatrix} = m^* \begin{pmatrix} \cos(\alpha(t) - \alpha_1^*(t)) \\ \sin(\alpha_1(t) - \alpha_1^*(t)) \end{pmatrix} \tag{20}$$

Thus, (7) and (11) remain valid, but with the vector π and its components p_c and p_s becoming functions of time. For small frequency error, the disturbance vector π slowly rotates in the two-dimensional space. This creates a drift of x with time causing a bursting of the control signal $u(t)$ and of the error $e(t)$. This demonstrates the necessity of obtaining an accurate estimate of the disturbance frequency.

IV. Use of frequency estimation

4.1. Magnitude/phase-locked loop frequency estimator

First assume that the control signal is equal to zero. Then, the output $y(t)$ is equal to the disturbance, which is assumed to be of the form (2). The algorithm reconstructs estimates $m(t)$, $\alpha_1(t)$ and $\omega_1(t)$ that yield an estimate of the output of the plant

$$\hat{y}(t) = m(t)\cos(\alpha_1(t)) \tag{21}$$

Defining the signal estimation error

$$e(t) = y(t) - \hat{y}(t) \tag{22}$$

and the vector

$$\begin{pmatrix} e_c(t) \\ e_s(t) \end{pmatrix} = 2\begin{pmatrix} \cos(\alpha_1(t)) \\ -\sin(\alpha_1(t)) \end{pmatrix} e(t) \tag{23}$$

the rest of the MPLL algorithm is given in the Laplace domain by

$$\begin{aligned} m(s) &= \frac{g_m}{s} e_c(s) \\ \omega_1(s) &= \frac{g_\omega}{s} e_s(s) \\ \alpha_1(s) &= \frac{ks+1}{s}\omega_1(s) \end{aligned} \tag{24}$$

where g_m, g_ω, and k are positive constants [2]. Note that (6) is now replaced by

$$\alpha_1(t) = k\omega_1(t) + \int_0^t \omega_1(\tau)d\tau \tag{25}$$

Other equations remain the same and, except for a bias, the phase estimate α_1 is the integral of the frequency estimate in steady-state. The benefit of a nonzero k will become obvious later. In [11], it was shown that a linearized approximation of 24 is stable for all positive values of the design parameters k, g_ω g_m.

4.2. Interaction of MPLL with ADHSS algorithm

With a control input of the from (4), (23) becomes

$$AVE\left[\begin{pmatrix} e_c \\ e_s \end{pmatrix}\right] = \begin{pmatrix} m^*\cos(\alpha_1 - \alpha_1^*) - m \\ m^*\sin(\alpha_1^* - \alpha_1) \end{pmatrix} + \begin{pmatrix} x_1^*\theta_c + x_2^*\theta_s \\ x_2^*\theta_c - x_1^*\theta_s \end{pmatrix} \tag{26}$$

As such, the linearized system is described by the same characteristic polynomials and is stable under the same conditions. Further, as long as the control signal is at the MPLL frequency, it is rejected by the MPLL. Nevertheless, there is a catch, in that the equilibrium state is shifted and m and α_1 satisfy different nonlinear equations

$$\begin{aligned} m - m^*\cos(\alpha_1 - \alpha_1^*) &= x_1^*\theta_c + x_2^*\theta_s \\ m^*\sin(\alpha_1 - \alpha_1^*) &= x_1^*\theta_s - x_2^*\theta_c \end{aligned} \tag{27}$$

Note that $m(t)$ is an estimate of the magnitude of $y(t)$ and, due to the control signal, not an estimate of m^*.Therefore, a new necessary and sufficient condition for the existence of an equilibrium of the MPLL is that

$$\left|\frac{x_2^*\theta_c - x_1^*\theta_s}{m^*}\right| < 1 \tag{28}$$

In other words, the effect of the control signal on the output must not be greater than the disturbance magnitude for phase-lock to be possible.

Also, (27) and (20) indicate that, if phase-lock occurs,

$$-P_I\theta_c + P_R\theta_s + p_s = 0 \tag{29}$$

This equation is the second equation of $G\theta + \pi = 0$, which guarantees perfect disturbance cancellation.The first equation is

$$P_R\theta_c + P_I\theta_s + p_c = 0 \tag{30}$$

and does not involve p_s. In other words, cancellation of the disturbance can be achieved in a combined algorithm regardless of x_4, the estimate of p_s. In particular, the parameter x_4 can be set to zero, which is equivalent to assuming that $p_s = 0$. In reality, p_s is not zero, but the phase of the MPLL converges to a value such that one may make this assumption in the ADHSS. For this reason, we now consider an ADHSS algorithm with 3 parameters instead of 4, *i.e.,* an ADHSS algorithm that assumes a known phase of the disturbance signal.

4.3. ADHSS with known frequency and phase

The ADHSS algorithm for known phase is obtained by dropping the parameter x_4 in the previous algorithm so that x is now a column vector with only 3 elements. The result is a simpler algorithm. The vector of control parameters becomes

$$\theta(x) = \begin{pmatrix} \theta_c(x) \\ \theta_s(x) \end{pmatrix} = -\frac{1}{x_1^2 + x_2^2}\begin{pmatrix} x_1x_3 \\ x_2x_3 \end{pmatrix}. \tag{31}$$

The vector of unknowns is

$$x^* = \begin{pmatrix} P_R & P_I & m^* \end{pmatrix}^T \tag{32}$$

and the regressor used for adaptation is

$$W(t,\theta) = E(x)w_1(t) \tag{33}$$

where

$$E(x) = \begin{pmatrix} \theta_c(x) & \theta_s(x) & 1 \\ \theta_s(x) & -\theta_c(x) & 0 \end{pmatrix}^T \tag{34}$$

Other equations of the algorithm remain the same as Sec. 3.1. Averaging theory can be used to analyze this system as in [8]. The averaged system corresponding to the adaptive system is simply

$$\dot{x} = -\frac{g}{2}E(x)E^T(x)\,(x - x^*) \tag{35}$$

4.3.1. Equilibrium subset

It can be shown that the equilibrium set can be parameterized as a function of a single variable. For example, if $x_1^* \neq 0$, one can express x_2 and x_3 as functions of x_1 with

$$x_2 = \frac{x_2^* x_1}{x_1^*}, \quad x_3 = \frac{x_3^* x_1}{x_1^*} \tag{36}$$

In general, the set of equilibrium points is a line connecting the origin of the three-dimensional state-space and the nominal parameter x^*. Any equilibrium of the averaged system is also an equilibrium of the original system. It can also be shown that equilibrium points as described by (36) are such that

$$\begin{pmatrix} \theta_c(x) \\ \theta_s(x) \end{pmatrix} = -\frac{1}{x_1^{*2} + x_2^{*2}} \begin{pmatrix} x_1^* x_3^* \\ x_2^* x_3^* \end{pmatrix} = \begin{pmatrix} \theta_c^* \\ \theta_s^* \end{pmatrix} \tag{37}$$

In other words, an equilibrium point corresponds to a control parameter vector equal to the nominal one, and results in exact cancellation of the disturbance.

4.3.2. Local stability of equilibrium points

Linearizing (35) with (34) around an equilibrium state x, the following eigenvalues can be computed

$$\begin{aligned} \lambda_1 &= 0, \quad \lambda_2 = -g\frac{x_i^*}{x_i}\frac{x_3^{*2}}{x_1^{*2} + x_2^{*2}}, \\ \lambda_3 &= -g\frac{x_i^*}{x_i}\left(1 + \frac{x_3^{*2}}{x_1^{*2} + x_2^{*2}}\right) \end{aligned} \tag{38}$$

where $i = 1, 2,$ or 3 (whichever corresponds to a nonzero x_i) Thus, the condition for stability of an equilibrium point is that

$$\text{sign}(x_i) = \text{sign}(x_i^*) \tag{39}$$

which means that the equilibrium point is stable if it is on the same side of the origin as the nominal parameter x^*. A corresponding orthogonal set of eigenvectors is given by

$$\begin{aligned} v_1 &= \begin{pmatrix} x_1^* \\ x_2^* \\ x_3^* \end{pmatrix}, v_2 = \begin{pmatrix} -x_2^* \\ x_1^* \\ 0 \end{pmatrix}, \\ v_3 &= \begin{pmatrix} x_1^* x_3^* \\ x_2^* x_3^* \\ -x_1^{*2} - x_2^{*2} \end{pmatrix} \end{aligned} \tag{40}$$

Note that $|\lambda_2| < |\lambda_3|$ and may be much smaller if $x_3^{*2} \ll x_1^{*2} + x_2^{*2}$. In such cases, convergence of the state x_3 (the estimate of the disturbance magnitude) occurs fast, followed by a slower convergence within the $x_1 - x_2$ plane.

4.3.3. Trajectories of the averaged system

Consider the following assumption.

Assumption 1 Assume that trajectories of the original and averaged system are such that $x_1^2 + x_2^2 \geqslant \delta$ for some $\delta > 0$.

Using the Lyapunov function $v = \|x(t) - x^*\|^2$, one finds that $\dot{v} \leq 0$ and

$$\|x(t) - x^*\| \leq \|x(0) - x^*\| \tag{41}$$

Since x and $\dot{x}$ are bounded (using (35) and Assumption 1) and $E^T(x)x^* = 0$, one may deduce that $E^T(x)\,(x - x^*) \to 0$ as $t \to \infty$, and therefore the equilibrium line is reached and the disturbance is asymptotically cancelled. Using $v = \|x(t)\|^2$, one finds that $\dot{v} = 0$, so that

$$\|x(t)\| = \|x(0)\| \tag{42}$$

for all t. Because all trajectories converge to the equilibrium line, the steady-state value of x must satisfy (36) as well as (42). Combining the equations, one gets the remarkable property that, asymptotically

$$x_i = x_i^*\frac{\|x(0)\|}{\|x^*\|}, \quad \text{for all } i \tag{43}$$

The reverse sign is also allowed by the equations, but the stability property determines that the positive sign must be used. Thus, trajectories of x travel along the sphere that is centered at the origin and includes $x(0)$, and eventually converge to the intersection of the sphere with the line connecting the origin to x^*, on the same side as x^*.

4.3.4. Illustrative simulations

The simulation highlights the stability properties of the adaptive system. The disturbance frequency is now $\omega_1^* = 320\pi$. The plant is the same, the adaptive gain $g = 100$ and

$$x^* = \begin{pmatrix} 0.7471 & .1548 & 0.1 \end{pmatrix}^T \tag{44}$$

The initial vector is

$$x(0) = \begin{pmatrix} -1 & 1 & 0 \end{pmatrix}^T \tag{45}$$

and corresponds to an initial estimate of the phase of the plant

$$\tan^{-1}(x_2(0)/x_1(0)) = 135^o \tag{46}$$

while the actual phase of the plant is

$$\tan^{-1}(x_2^*/x_1^*) = \measuredangle P(j\omega_1^*) = 11.7^o \tag{47}$$

The phase difference of 123.3^o is beyond the 90^o angle condition. The state trajectory can be seen in Fig. 2. Although initially diverging from the unstable half of the line, the trajectory eventually reaches the stable side. As predicted from the stability analysis, there is a slower mode of convergence within the $x_1 - x_2$ plane that corresponds to a near constant value of x_3. Although not shown, it was verified that $\|x(t)\| = \|x(0)\|$.

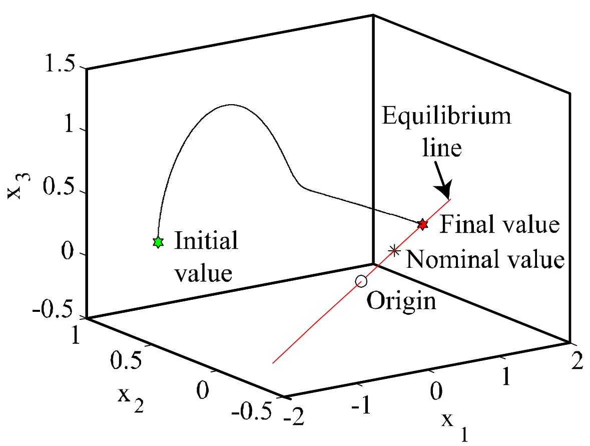

Fig. 2: State trajectory and relation to the line equilibrium..

V. Adaptive algorithm with unknown frequency and unknown plant

5.1. Adaptive algorithm and averaged system

The algorithm for the general problem of unknown frequency and plant is obtained by combining the MPLL algorithm with the (reduced) ADHSS algorithm for known phase and frequency, resulting in the differential equations

$$\begin{aligned}
\dot{x} &= -gE(x)w_1(t)\left(w_1^T(t)E^T(x)x - y\right) \\
\dot{m} &= 2g_m \cos(\alpha_1)(y - m\cos(\alpha_1)) \\
\dot{\omega}_1 &= -2g_\omega \sin(\alpha_1)(y - m\cos(\alpha_1)) \\
\dot{\alpha}_1 &= \omega_1 - 2kg_\omega \sin(\alpha_1)(y - m\cos(\alpha_1))
\end{aligned} \tag{48}$$

with positive constants g, g_m, g_ω, and k, and the algebraic equations (4), (31), and (34) with

$$w_1(t) = \begin{pmatrix} \cos(\alpha_1(t)) \\ \sin(\alpha_1(t)) \end{pmatrix} \tag{49}$$

Taking A, B, and C to be the matrices of a minimal state-space realization of the plant, so that $P(s) = C(sI - A)^{-1}B$, the overall equations describing the system are given by

$$\begin{aligned}
\dot{x}_P &= Ax_P + Bu = Ax_P + Bw_1^T(t)\theta(x) \\
y &= Cx_P + m^*\cos(\alpha_1^*) \\
&= Cx_P + m^*w_1(t)\begin{pmatrix} \cos(\alpha_1 - \alpha_1^*) \\ \sin(\alpha_1 - \alpha_1^*) \end{pmatrix} \\
\dot{\alpha}_1^* &= \omega_1^*
\end{aligned} \tag{50}$$

The overall system is described by complex, nonlinear time-varying differential equations. Again, averaging theory presents the best prospect for an approximation that would give insight into the dynamics of the system. The two components of the controller were already studied using averaging and were shown to possess desirable stability properties. It remains to show that their combination, including coupling effects, does not produce undesirable interactions (at least close to the nominal operating mode).

In previous analyses, the effect of the ADHSS on the MPLL was included in the averaging analysis, but the effect of a phase error on the known phase ADHSS was not. A correction term must be added in the averaged system, similar to what was done to study the effect of a frequency error on the 4-parameter ADHSS algorithm. Since

$$p(t) = m^*w_1^T(t)\begin{pmatrix} \cos(\alpha_1 - \alpha_1^*) \\ \sin(\alpha_1 - \alpha_1^*) \end{pmatrix} \tag{51}$$

instead of

$$p(t) = m^* \cos(\alpha_1) \tag{52}$$

the correction term to be added to the steady-state output is

$$\Delta y_{ss} = m^* w_1^T(t) \begin{pmatrix} \cos(\alpha_1 - \alpha_1^*) - 1 \\ \sin(\alpha_1 - \alpha_1^*) \end{pmatrix} \tag{53}$$

Adding the correction term to $y_{ss}$and substituting $\delta\alpha_1 = \alpha_1 - \alpha_1^*$, and $\delta\omega_1 = \omega_1 - \omega_1^*$, the overall averaged system becomes

$$\begin{aligned} \dot{x} &= -\frac{g}{2} E(x) E^T(x) (x - x^*) \qquad (54) \\ &\quad + \frac{g}{2} m^* E(x) \begin{pmatrix} \cos(\delta\alpha_1) - 1 \\ \sin(\delta\alpha_1) \end{pmatrix} \\ \dot{m} &= g_m (m^* \cos(\delta\alpha_1) - m + x_1^*\theta_c + x_2^*\theta_s) \\ \delta\dot{\omega}_1 &= -g_\omega (m^* \sin(\delta\alpha_1) - x_2^*\theta_c + x_1^*\theta_s) \\ \delta\dot{\alpha}_1 &= \delta\omega_1 - k g_\omega (m^* \sin(\delta\alpha_1) - x_2^*\theta_c + x_1^*\theta_s) \end{aligned}$$

5.2. Equilibrium points

Since $E^T(x)x = 0$, the equilibrium points are determined by

$$\begin{aligned} E^T(x)x^* + m^* \begin{pmatrix} \cos(\delta\alpha_1) - 1 \\ \sin(\delta\alpha_1) \end{pmatrix} &= 0 \qquad (55) \\ m^* \cos(\delta\alpha_1) - m + x_1^*\theta_c + x_2^*\theta_s &= 0 \qquad (56) \\ m^* \sin(\delta\alpha_1) - x_2^*\theta_c + x_1^*\theta_s &= 0 \qquad (57) \\ \delta\omega_1 &= 0 \qquad (58) \end{aligned}$$

Expanding (55) and using $x_3^* = m^*$, one finds that (55) is equivalent to

$$\begin{aligned} \theta_c x_1^* + \theta_s x_2^* + m^* \cos(\delta\alpha_1) &= 0 \qquad (59) \\ \theta_s x_1^* - \theta_c x_2^* + m^* \sin(\delta\alpha_1) &= 0 \qquad (60) \end{aligned}$$

(56) and (59) imply that the disturbance is cancelled. (57) and (60) are identical, which means that the equilibrium set, instead of being one-dimensional is actually two-dimensional, similar to the 4-parameter ADHSS.

Using the expression for (31), the conditions for the equilibrium points can be written as

$$\begin{aligned} x_3 \frac{x_1 x_1^* + x_2 x_2^*}{x_1^2 + x_2^2} &= m^* \cos(\delta\alpha_1) \\ x_3 \frac{x_2 x_1^* - x_1 x_2^*}{x_1^2 + x_2^2} &= m^* \sin(\delta\alpha_1) \qquad (61) \end{aligned}$$

If we define $\|P\|$, $\|P^*\|$, ϕ, and ϕ^* so that

$$\begin{aligned} x_1 &= \|P\| \cos(\phi) \\ x_2 &= \|P\| \sin(\phi) \qquad (62) \end{aligned}$$

and

$$\begin{aligned} x_1^* &= \|P^*\| \cos(\phi^*) \qquad (63) \\ x_2^* &= \|P^*\| \sin(\phi^*) \qquad (64) \end{aligned}$$

the conditions become

$$\begin{aligned} x_3 \frac{\|P^*\| \cos(\phi - \phi^*)}{\|P\|} &= m^* \cos(\delta\alpha_1) \\ x_3 \frac{\|P^*\| \sin(\phi - \phi^*)}{\|P\|} &= m^* \sin(\delta\alpha_1) \qquad (65) \end{aligned}$$

Due to the two-dimensional nature of the equilibrium subset, one can pick two free variables. If we pick $\|P\|$ and ϕ, x_1 and x_2 are given by (62) and $\delta\alpha_1$ and x_3 can take one of two possible values

$$\begin{aligned} \delta\alpha_1 &= \phi - \phi^* + n\pi \\ x_3 &= (-1)^n \, m^* \frac{\|P\|}{\|P^*\|} \qquad (66) \end{aligned}$$

with $n = 0$ or 1. Note that, for $n = 0$, the estimate of the magnitude of the disturbance is correct and the PLL phase error is zero if the estimate of the plant is exact. In general, the estimate of the magnitude of the disturbance is weighted by the ratio of the plant magnitude to the plant magnitude estimate, and the PLL phase error is equal to the plant phase error $\phi - \phi^*$. For $n = 1$, the magnitude estimate changes sign and the phase simply shifts by $180°$ to compensate for it.

5.2.1. Local stability of equilibrium points

The local stability of the equilibrium points can be obtained by linearizing (54) around an equilibrium state. This computation and others to follow are best performed using a symbolic computation engine. Allowing J to denote the Jacobian of the system evaluated around an equilibrium, the characteristic equation of the linearized system $\det(\lambda I - J) = 0$ has the following form

$$\lambda^2 (\lambda + g_m) \left(c_3 \lambda^3 + c_2 \lambda^2 + c_1 \lambda + c_0 \right) = 0. \tag{67}$$

The 2 eigenvalues at $\lambda = 0$ are associated with the two-dimensional equilibrium subset, and the stable eigenvalue at $\lambda = -g_m$ is associated with the state m, which depends on but does not influence other states. The stability of the three remaining eigenvalues can be ascertained by considering the third-order polynomial with coefficients

$$
\begin{aligned}
c_3 &= 1 \\
c_2 &= \cos(\phi - \phi^*) \left(g a_1 + \frac{1}{2} g a_4 + (-1)^n 2 k g_\omega m^* \right) \\
c_1 &= (-1)^n \frac{1}{2} g k g_\omega m^* (a_1 + a_4) + \frac{g^2}{4} (a_1^2 + a_2^2) \\
&\quad + (-1)^n g_\omega m^* \cos(\phi - \phi^*) \\
c_0 &= (-1)^n \frac{1}{2} g g_\omega m^* (a_1 + a_4) \qquad (68)
\end{aligned}
$$

where

$$a_1 = \frac{m^{*2}}{\|P\| \|P^*\|}, \quad a_2 = \frac{m^*}{\|P\|} \qquad (69)$$

$$a_3 = \frac{m^{*2}}{\|P^*\|}, \quad a_4 = \frac{\|P^*\|}{\|P\|} \qquad (70)$$

By application of the Routh-Hurwitz test [7], when $n = 1$, c_0 is negative indicating there are always eigenvalues in the right-half plane. If $n = 0$,.the stability of the system is guaranteed if and only if

$$|\phi - \phi^*| < 90^\circ \text{ and } c_2 c_1 - c_3 c_0 > 0 \qquad (71)$$

The condition $c_2 c_1 - c_3 c_0 > 0$ is equivalent to

$$\cos^2(\phi - \phi^*) + b_1 \cos(\phi - \phi^*) - b_0 > 0 \qquad (72)$$

where (reintroducing the original variables)

$$
\begin{aligned}
b_1 &= g \left(\|P^*\|^2 + m^{*2} \right) \frac{2 k g_\omega \|P\| \|P^*\| + g m^*}{4 g_\omega \|P\|^2 \|P^*\|^2} \qquad (73) \\
b_0 &= \frac{g \left(\|P^*\|^2 + m^{*2} \right)}{g \left(\|P^*\|^2 + m^{*2} \right) + g m^{*2} + 2 k g_\omega m^* \|P\| \|P^*\|}
\end{aligned}
$$

Therefore, (71) is satisfied if and only if

$$|\phi - \phi^*| < \bar{\phi} \qquad (74)$$

where

$$\bar{\phi} = \cos^{-1} \left(\frac{\sqrt{b_1^2 + 4 b_0} - b_1}{2} \right) \qquad (75)$$

$\bar{\phi}$ is well-defined and less than 90° because $b_1 > 0$ and $1 > b_0 > 0$.

In conclusion, there is always a positive range of angle ϕ around the nominal angle ϕ^* for which the system is stable. The range is reduced from the previous range of $\pm 90^\circ$. It depends in a complicated manner on the system parameters, and also on the location on the equilibrium surface through the parameter $\|P\|$. The range becomes $\pm 90^\circ$ again if $b_0 \to 0$ or $b_1 \to \infty$. This condition is guaranteed as $k \to \infty$. Thus, for k chosen sufficiently large, the stability region of the averaged system approaches the same region as the ADHSS with known frequency.

VI. Experiments

The performance of the algorithm was examined through single-channel active noise control experiments. The algorithm was coded in C and implemented in a dSpace DS1104 digital signal processing board. A sampling frequency of 8 kHz was used. A constant amplitude sinusoidal disturbance with frequency of 180 Hz was generated by a loudspeaker, while the control signal was produced by another loudspeaker. A microphone was used to measure the cancellation error. The plant consists of the hardware and transmission in the environment from the control signal output to the error microphone input. The experiments were conducted in a small room where many signal reflections are present. This is a challenging problem that helps to illustrate the performance of the algorithm in difficult conditions. The gain

$$g = \begin{pmatrix} 100 & 0 & 0 \\ 0 & 100 & 0 \\ 0 & 0 & 1 \end{pmatrix} \qquad (76)$$

was used.

6.1. Experiments with disturbances of time-varying magnitude

In the following experiment, the frequency of the disturbance and the plant were fixed, but the magnitude of the disturbance m^* varied significantly. Results are shown where the disturbance goes away in three steps. The goal of the experiment is to study the implications of the phase-lock condition (28) for the combined ADHSS/MPLL algorithm. (28) suggests that phase-lock could be lost when the m^* suddenly decreases. However, the results show that the nonlinear dynamics of the combined algorithm are able to adjust the estimated parameters in such a way that phase-lock as well as significant disturbance rejection are maintained. Fig. 3 shows the disturbance, whose magnitude goes away and then returns to its value roughly 1 second later. The control signal changes in equal proportion, and disturbance cancellation is maintained. Fig. 4 shows the states of the adaptive HSS. As one would expect, the decrease in m^* is reflected primarily in x_3. Fig. 5 shows the frequency estimate ω_1. From the oscillations in the frequency estimate of Fig. 5, it is observed that the MPLL does not loose phase-lock until the disturbance has gone completely away.

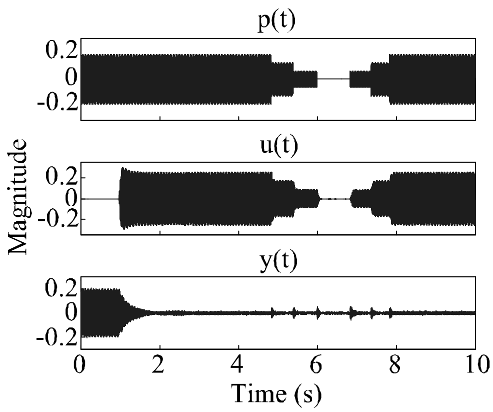

Fig. 3: Disturbance, control signal, and the output of the plant when the disturbance goes away in three steps and then comes back.

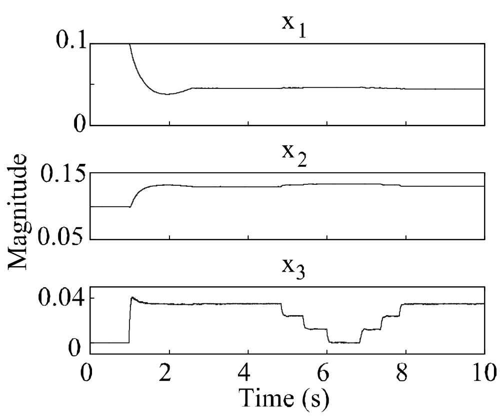

Fig. 4: The states of the adaptive HSS when the disturbance goes away in three steps and then comes back.

6.2. Experiments with disturbances of time-varying frequency

In the next experiment, the ability to deal with a step change in the disturbance frequency was investigated. Once the system reached steady-state, the disturbance frequency was abruptly changed from $180Hz$ to $185Hz$. Fig. 6 shows the frequency estimate, which tracks the sudden change in the disturbance frequency. Fig. 7 shows the output of the plant. When the disturbance frequency changes, we note a small spike in $y(t)$. However, the system quickly recovers, and significant disturbance rejection is maintained.

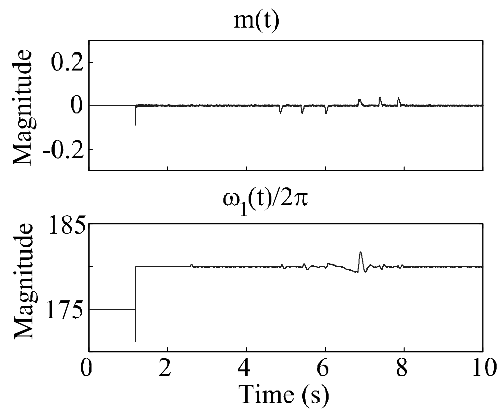

Fig. 5: The MPLL frequency estimate when the disturbance goes away in three steps and then comes back.

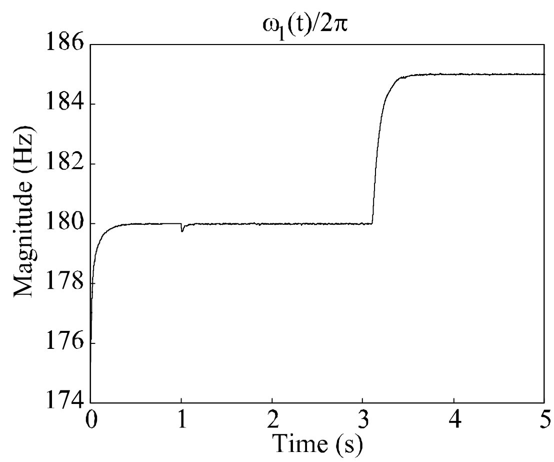

Fig. 6: Frequency estimate when the disturbance frequency is stepped from $180Hz$ to $185Hz$.

VII. Conclusions

An adaptive algorithm for the rejection of a sinusoidal disturbance of unknown/time-varying frequency acting at the output of an unknown/time-varying plant was presented. The algorithm had a disturbance rejection component based on an adaptive harmonic steady-state algorithm that estimates the plant frequency response at the disturbance frequency along with the disturbance parameters. Because this component required that the frequency be known exactly, a second component providing frequency estimation was added. It was found that the magnitude/phase-locked loop algorithm used for frequency estimation

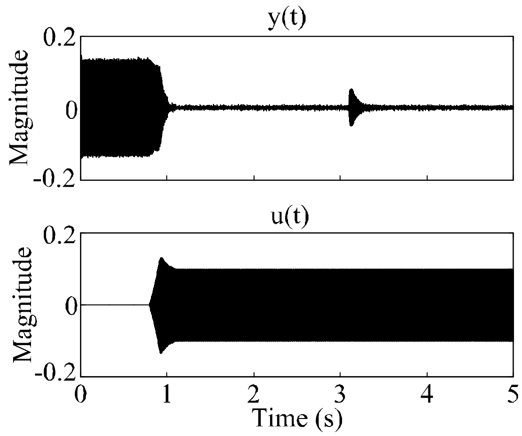

Fig. 7: The plant output and control signal when the disturbance frequency is stepped from $180Hz$ to $185Hz$.

was able to deal with the effect of the control signal on the plant output. Further, its properties enabled the simplification of the ADHSS algorithm. Under steady-state approximations, the MPLL is known to be locally stable, while the ADHSS is globally stable.

The combination of the ADHSS and MPLL resulted in an overall system described by 6 nonlinear time-varying differential equations. The theory of averaging was applied to find that the equilibrium of the system was a two-dimensional surface. Any point on the surface resulted in cancellation of the disturbance. An eigenanalysis of the averaged system linearized around the equilibrium surface revealed that a subset of the surface was locally stable. Various ANC experiments demonstrated the ability of the algorithm to track variations in both system and disturbance parameters. A two-phase start-up procedure was used to be sure that the stable subset of the equilibrium surface was reached.

VIII. List of symbols

The following symbols were used in the paper: $y(t)$, $u(t)$, $p(t)$, $P(s)$, P_R, P_I, $w_1(t)$, π, θ, θ_C, θ_S, θ^*, θ_C^*, θ_S^*, $\alpha_1(t)$, α_1^*, $\omega_1(t)$, ω_1^*, $m(t)$, m^*, G, $W(t,\theta)$, $x(t)$, x_i, x^*, x_i^*, e. e_c, e_s, λ_i, v_i, x_P, A, B, C, Δys_s $\delta\alpha_1$, $\delta\alpha_1^*$, $\delta\omega_1$, $\delta\omega_1^*$, c_i, b_i, ϕ, ϕ^*, $\bar{\phi}$, g, g_ω, g_m, k.

REFERENCES

1. X. Guo & M. Bodson, ”Adaptive rejection of disturbances having two sinusoidal components with close and unknown frequencies,” *Asian Journal of Control*.doi: 10.1002/asjc.285 (2010).
2. X. Guo & M. Bodson, ”Analysis and Implementation of an Adaptive Algorithm for the Rejection of Multiple Sinusoidal Disturbances,” *IEEE Trans. on Control Systems Technology*, vol. 17, no. 1, pp. 40-50(2009).
3. C. Chung, M. Chen, and A. Hsue, "A new adaptive control for periodic tracking/disturbance rejection," *Asian Journal of Control*. doi: 10.1002/asjc.409 (2011).
4. S. M. Kuo & D. Vijayan, ”A Secondary Path Modeling Technique for Active Noise Control Systems,” *IEEE Trans. on Speech and Audio Processing*, vol. 5, no. 4, pp. 374-377(1997).
5. M. Niedzwiecki & M. Meller, "A New Approach to Active Noise and Vibration Control-Part I: The Known Frequency Case," *IEEE Trans. Signal Processing*, vol. 57, no. 9, pp. 3373 -3386(2009).
6. M. Niedzwiecki & M. Meller, "A New Approach to Active Noise and Vibration Control-Part II: The Unknown Frequency Case," *IEEE Trans. Signal Processing*, vol. 57, no. 9, pp. 3387 -3398(2009).
7. C. Phillips & R. Harbor, *Feedback Control Systems*, Prentice Hall, Upper Saddle River, New Jersey(2000).
8. S. Pigg and M. Bodson, "Adaptive Algorithms for the Rejection of Sinusoidal Disturbances Acting on Unknown Plants," *IEEE Trans. on Control System Technology*, vol. 18, no. 4, pp. 822-836(2010).
9. S. Sastry and M. Bodson, *Adaptive Control: Stability, Convergence, and Robustness*, Prentice Hall, Englewood Cliffs,New Jersey(1989).
10. Y. Song, Y. Gong, & S. M.Kuo, “A Robust Hybrid Feedback Active Noise Cancellation Headset,” *IEEE Transactions on Speech and Audio Processing*, vol. 13, no. 4, pp. 607-617(2005).
11. B. Wu and M. Bodson, "A Magnitude/Phase-locked Loop Approach to Parameter Estimation of Periodic Signals," *IEEE Trans. on Automatic Control*, vol. 48, no. 4, pp. 612-618(2003).
12. Y. Xiao, L. Ma, & K. Hasagawa, "Properties of FXLMS-Based Active Noise Control with Online Secondary Path Modeling," *IEEE Trans. Signal Processing*, vol. 57, no. 8, pp. 2931-2949(2009).
13. M. Zhang, H. Lan, & W. Ser, ”An Improved Secondary Path Modeling Method for Active Noise Control Systems,” *IEEE Signal Processing Letters*, vol. 7, no. 4, pp. 73-75(2000).